EDGE ARTICLE

Check for updates

Chemical synthesis of stimuli-responsive guide RNA for conditional control of CRISPR-Cas9 gene editing†

Chunmei Gu, Lu Xiao, Jiachen Shang, Xiao Xu, Luo He and Yu Xiang [ID] *

CRISPR-Cas9 promotes changes in identity or abundance of nucleic acids in live cells and is a programmable modality of broad biotechnological and therapeutic interest. To reduce off-target effects, tools for conditional control of CRISPR-Cas9 functions are under active research, such as stimuli-responsive guide RNA (gRNA). However, the types of physiologically relevant stimuli that can trigger gRNA are largely limited due to the lack of a versatile synthetic approach in chemistry to introduce diverse labile modifications into gRNA. In this work, we developed such a general method to prepare stimuli-responsive gRNA based on site-specific derivatization of 2′-*O*-methylribonucleotide phosphorothioate (PS-2′-OMe). We demonstrated CRISPR-Cas9-mediated gene editing in human cells triggered by oxidative stress and visible light, respectively. Our study tackles the synthetic challenge and paves the way for chemically modified RNA to play more active roles in gene therapy.

1. Introduction

CRISPR-Cas (clustered regularly interspaced short palindromic repeats, CRISPR-associated genes),[1] initially discovered as a bacterial adaptive immune system, has become the new frontier for genome engineering in eukaryotes including humans.[2–4] In addition to delivery of DNA that encodes the guide RNA (gRNA) and Cas9 protein using lipid nanoparticles or recombinant viruses,[5,6] efficient genome editing has also been observed with ribonucleoprotein (RNP) and mRNA delivery.[7,8] As RNA usually has a shorter half-life compared to DNA, these delivery methods are often associated with considerably lower off-target effects.[9,10] For this purpose, chemically modified gRNA,[11–15] either in the form of a single guide RNA (sgRNA)[11] or a two-component CRISPR RNA (crRNA) and *trans*-activating crRNA (tracrRNA),[12] is actively studied.

To facilitate precise intracellular applications such as gene editing and regulation, conditional control of gRNA activities has been achieved through equipping the RNA oligonucleotides with stimuli-responsive modifications, including those sensitive to ultraviolet (UV) light,[16–30] redox conditions,[31,32] and bioorthogonal chemicals.[33–35] These modifications can be introduced into RNA *via* the ribose 2′-OH,[18,24–26,31,34–37] nucleobases,[17,21,27–29] and internal or terminal linkers.[19,20,22,23,30,33,38]

They can perturb the native gRNA structures, thereby abrogating the CRISPR-Cas functions. The caged gRNA activities can then be restored by subsequent removal of labile modifications when encountering stimuli of interest. Gene editing responsive to light and chemicals were demonstrated using these powerful tools made of stimuli-responsive gRNA,[16–35] distinguished from other strategies based on protein engineering[39,40] or functional modulation through riboswitches[41–43] and RNA hybridization.[44]

Despite the great promise, currently available stimuli-responsive gRNA can only respond to a limited number of physiologically relevant stimuli, due to the lack of a general method to introduce a broad range of labile modifications into gRNA.[45,46] For example, reactive oxygen species (ROS) that are important signaling molecules related to diseases[47–49] and visible light that is less cytotoxic than UV light for spatiotemporal manipulation, still cannot serve as efficient triggering signals to activate gRNA functions due to the synthetic difficulties. Although strategies to introduce ROS-labile phenylboronate (BO) and visible light-labile aminocoumarin (CM) have been demonstrated for DNA oligonucleotides,[17,50–52] they are unsuccessful in functionalizing RNA. BO is incompatible with the fluoride treatment used in RNA solid-phase synthesis for deprotecting the silyl ether at the ribose 2′-OH because of forming strong B–F bonds.[53,54] Enzymatic incorporation of visible light-labile groups was demonstrated using tRNA guanine transglycosylases through a 17-nt RNA oligonucleotide tag.[55,56] However, the activity of tRNA guanine transglycosylases is context-dependent and the method cannot be generalized to modify arbitrary RNA sequences.

Chemical properties of RNA ribose 2′-OH[18,24–26,31,34–37] and nucleobases[17,21,27–29] have been extensively studied for

Department of Chemistry, Beijing Key Laboratory for Microanalytical Methods and Instrumentation, Key Laboratory of Bioorganic Phosphorus Chemistry and Chemical Biology (Ministry of Education), Tsinghua University, Beijing 100084, China. E-mail: xiang-yu@tsinghua.edu.cn

† Electronic supplementary information (ESI) available: Experimental details and additional figures. See DOI: 10.1039/d1sc01194d

functional group incorporation. In contrast, RNA derivatization through the phosphodiester backbone is much less explored owing to the weak reactivity of native RNA phosphodiesters. Diazo-based reagents were initially reported to randomly modify RNA phosphodiesters without site specificity,[57] but were later identified to primarily react with nucleobases.[58] Phosphorothioate (PS) is a commercially available and low-cost modification that can be site-specifically installed in oligonucleotides through solid-phase synthesis.[59] Post-synthetic derivatization of PS can, therefore, enable incorporation of functional groups that are difficult for solid-phase synthesis of oligonucleotides, in a site-specific manner.[51,60–69] Previously, we demonstrated efficient PS derivatization for DNA modifications.[51,68,69] However, we found that directly reacting RNA phosphorothioate (PS-2′-OH)[70,71] with 4-bromomethylphenylboronic acid pinacol ester (BO–Br) did not afford any BO-modified RNA. Instead, a cyclic phosphotriester was formed likely *via* attacking the intermediate phosphorothiotriester by the proximate ribose 2′-OH, and it could be further hydrolyzed in buffers to yield RNA with a mixture of 3′–5′ and 2′–5′ phosphodiester linkages (Fig. S1 and S2, ESI†). We speculate that this side reaction caused by 2′-OH is the reason why the efficient PS derivatization has been widely applied to modify DNA,[51,60–69] but never used for RNA.

In this work, we developed a general method for synthesizing stimuli-responsive gRNA through site-specific derivatization of 2′-*O*-methylribonucleotide phosphorothioate (PS-2′-OMe) in the RNA (Scheme 1A). PS-2′-OMe modifications are already used in

FDA-approved oligonucleotide drugs, and usually do not disturb RNA functions such as small interfering RNA (siRNA) and gRNA.[11,12,14,72] Our method takes advantage of the clean reaction between PS-2′-OMe and arylmethylbromides (Aryl-Br) to attach labile groups to the RNA phosphodiester backbone (Scheme 1A), enabling caged RNA functions to be released when encountering stimuli of interest (Scheme 1B). To show the generality of aryl groups, we applied the strategy to incorporate BO and CM into the gRNA of the CRISPR-Cas9 system and demonstrated ROS- and visible light-triggered gene editing in human cells mediated by CRISPR-Cas9 (Scheme 1B and C). Bypassing direct modification through solid-phase synthesis, our strategy can be generally applied for site-specific functionalization of gRNA with various chemical groups.

2. Results and discussion

2.1. Chemistry for synthesizing stimuli-responsive RNA through PS-2′-OMe

To validate the phosphorothioate chemistry for RNA modification, we first took 20-nucleotide (20-nt) RNA oligonucleotides containing one or three adjacent PS-2′-OMe sites (1PS-2′-OMe-RNA or 3PS-2′-OMe-RNA) to react with BO-Br, and obtained the desired 1BO-RNA or 3BO-RNA almost quantitatively according to the polyacrylamide gel electrophoresis (PAGE) analyses (Fig. 1A). The identities of the BO-modified RNA were further confirmed by electrospray ionization-mass spectrometry (ESI-MS) characterizations (Fig. 1B, see Fig. S3a and b† for full
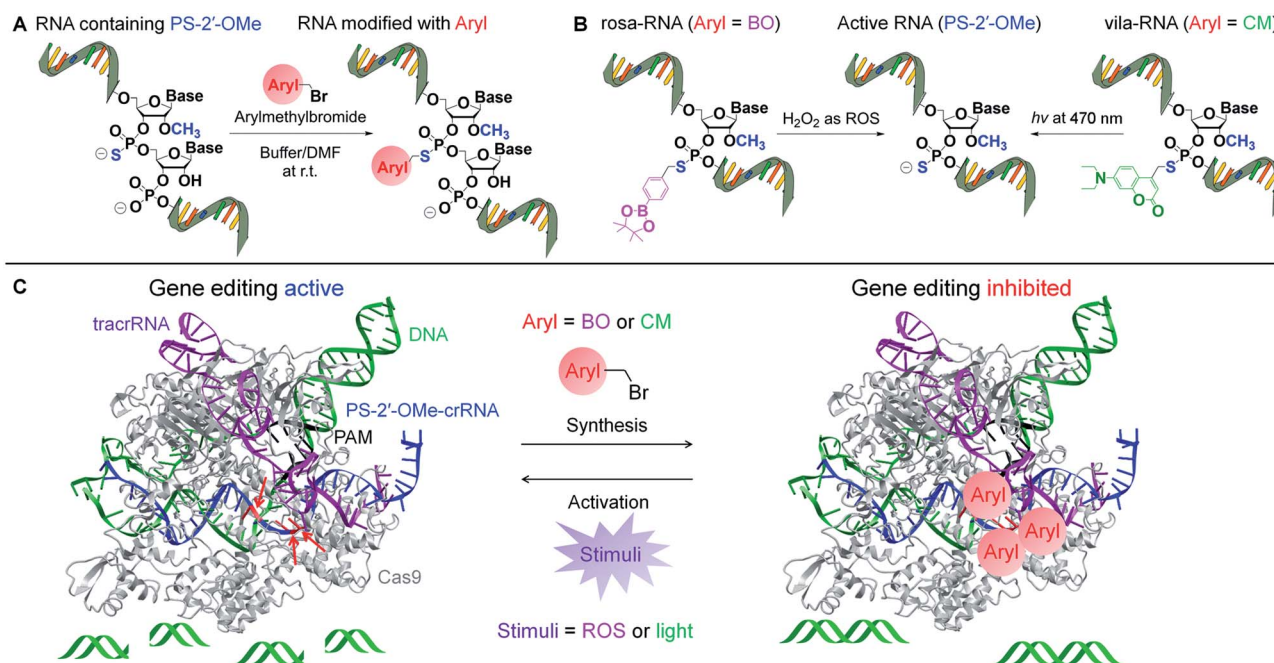
Scheme 1 General strategies for synthesis and conditional control of gRNA. (A) General method for RNA modification through site-specific derivatization of PS-2′-OMe. The reaction occurs at PS-2′-OMe without affecting any canonical RNA nucleotide. Aryl = aromatic groups; DMF = *N*,*N*-dimethylformamide; r.t. = room temperature. (B) ROS-activated RNA (rosa-RNA) and visible light-activated RNA (vila-RNA) synthesized by the general method using pinacol phenylboronate (BO) and *N*,*N*-diethylaminocoumarin (CM) as the aryl groups, respectively. RNA function is interrupted by BO or CM, and can be restored by applying H_2O_2 as ROS or visible light irradiation (*hv*) at 470 nm. (C) Conditional control of CRISPR-Cas9-mediated gene editing using stimuli-responsive gRNA prepared through the general method. ROS and visible light control is validated with BO-modified and CM-modified crRNA, respectively.
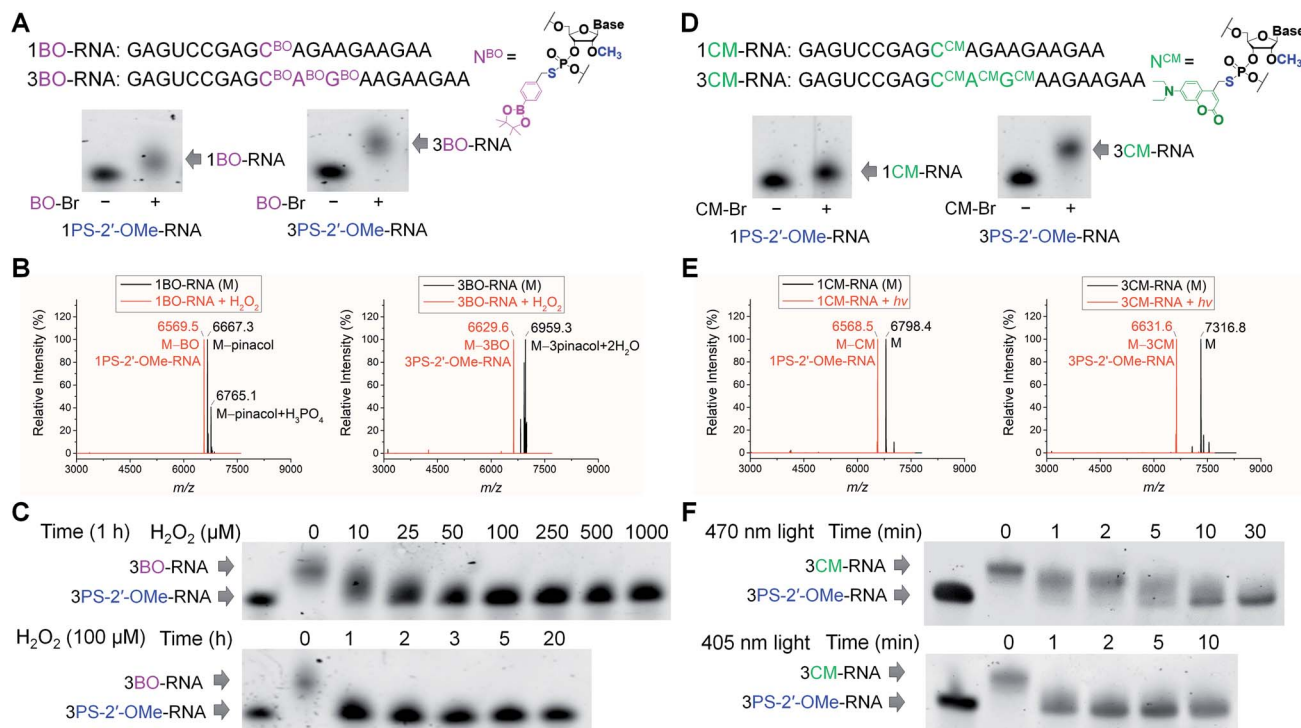
Fig. 1 Characterizations of stimuli-responsive RNA oligonucleotides. (A) Sequences of 1BO-RNA and 3BO-RNA containing the structure of BO-modified nucleotide (N^{BO}), and PAGE analyses of 1PS-2′-OMe-RNA and 3PS-2′-OMe-RNA reacted with or without BO-Br. (B) ESI-MS analyses of 1BO-RNA (left) and 3BO-RNA (right) before (black) and after (red) treatment of H_2O_2. (C) Dose- and time-dependent removal of BO from 3BO-RNA by H_2O_2. (D) Sequences of 1CM-RNA and 3CM-RNA containing the structure of CM-modified nucleotide (N^{CM}), and PAGE analyses of 1PS-2′-OMe-RNA and 3PS-2′-OMe-RNA reacted with or without CM-Br. (E) ESI-MS analyses of 1CM-RNA (left) and 3CM-RNA (right) before (black) and after (red) visible light irradiation. (F) Time-dependent removal of CM from 3CM-RNA by visible light irradiation at 470 nm (top) and 405 nm (bottom).

spectra). Hydrolysis of phenylboronic acid pinacol esters occurred during ionization in ESI-MS, so that peaks corresponding to molecules lacking the pinacol moieties were observed when analyzing BO-modified RNAs using ESI-MS.

We then set out to test whether BO modification in the RNAs can be removed by ROS (Scheme 1B). We treated 1BO-RNA and 3BO-RNA with hydrogen peroxide (H_2O_2), the most stable and major form of ROS and the indicator of cellular oxidative stress. ESI-MS analyses confirmed successful removal of BO and formation of 1PS-2′-OMe-RNA and 3PS-2′-OMe-RNA after H_2O_2 treatment (Fig. 1B), most likely through the mechanism shown in Scheme 1B. The BO removal reactions happened in a dose- and time-dependent manner (Fig. 1C). Full restoration of 3PS-2′-OMe-RNA was achieved by 25 μM H_2O_2 within 1 h. The H_2O_2 level in human cells under oxidative stress caused by amyloid β protein aggregation or hepatitis C infection was reported to reach 10–50 μM,[73–75] indicating that BO-modified RNA is promising for responding to intracellular H_2O_2 levels under the physiologically relevant conditions. We further confirmed that PS-2′-OMe was essential for BO derivatization, because replacing PS-2′-OMe by PS-2′-OH or native RNA backbone failed in the BO modification (Fig. S1 and S2†).

To obtain visible light-responsive RNA (Scheme 1B), we reacted 1PS-2′-OMe-RNA and 3PS-2′-OMe-RNA with 4-bromomethyl-7-diethylaminocoumarin (CM-Br). Quantitative formation of 1CM-RNA and 3CM-RNA was confirmed by PAGE (Fig. 1D) and ESI-MS (Fig. 1E, see Fig. S3c and d† for full spectra). Removal of CM promoted by light irradiation was also supported by ESI-MS (Fig. 1E). The reaction went to completion within 10 min when irradiated by visible light at a wavelength of 470 nm and an intensity of 13 mW cm^{-2} (Fig. 1F). When irradiation was carried out with the same intensity at 405 nm, the maximum absorption wavelength of CM, full removal of three CM modifications from 3CM-RNA finished in 1 min (Fig. 1F), indicating the light-induced reaction is robust and offers fast temporal control. Irradiation at 470 nm, although conferring slower CM removal than that at 405 nm, is less cytotoxic and can achieve wavelength-selective removal of CM over widely used UV-labile groups such as *o*-nitrobenzyl derivatives.[52]

2.2. Stimuli-responsive gRNA for ROS- and visible light-controlled CRISPR-Cas9 function *in vitro*

With the site-specific BO and CM derivatizations of PS-2′-OMe and their subsequent stimuli-responsive removal in RNA both validated, we sought to apply the ROS-activated RNA (rosa-RNA) and the visible light-activated RNA (vila-RNA) for conditionally controlled gene editing mediated by CRISPR-Cas9. According to the reported single-molecule studies, the 10-nt seed region in gRNA is critical for double-stranded DNA recognition by the Cas9/gRNA complex (Scheme 1C and Fig. 2A).[76] Therefore,

perturbation of this 10-nt seed region in crRNA by bulky modifications such as BO and CM is likely to abolish the gene-editing activities, for example, on the human EMX1 locus (Fig. 2A). Additionally, since crRNA nucleotides that can hybridize with tracrRNA remain unchanged, RNP complex should still form with crRNA, tracrRNA and Cas9 to ensure sufficient stability intracellularly.[2–4] We chose to introduce BO and CM into this 10-nt seed region of the 42-nt crRNA$_{EMX1}$ to block the gene-editing activities, as well as for their ROS- and visible light-controlled activations subsequently (Fig. 2A). Here we used crRNA (~40 nt) instead of sgRNA (~100 nt) for post-synthetic chemical modification, to avoid the difficulty in solid-phase synthesis of long RNA oligonucleotides containing PS-2′-OMe modifications.

We first screened a panel of different incorporation sites for PS-2′-OMe within the 10-nt seed region (AGAAGAAGAA), as shown in Fig. S4.† PS-2′-OMe was previously reported compatible with gRNA activities.[11,12,14] As a result, we expected PS-2′-OMe-modified crRNAs to have comparable activity with the unmodified crRNA. To our surprise, the gene-editing activity was found significantly dampened when PS-2′-OMe sites in crRNA$_{EMX1}$ were installed too close to the protospacer adjacent

motif (PAM) in the CRISPR-Cas9 complex (Fig. 2A). The PS-2′-OMe modification at site 19 for 3PS-2′-OMe-171819-crRNA$_{EMX1}$ (containing AGAAGAA^{m*}G^{m*}A^{m*}A, the seed region underlined, the PS-2′-OMe nucleotides indicated with superscripted m*, see Experimental section for full sequences) sharply reduced the activity, and PS-2′-OMe modification within site 21–25 for 3PS-2′-OMe-212223-crRNA$_{EMX1}$ (containing AGAAGAAGAA *G*^{m*}*U*^{m*}*U*^{m*}, additional nucleotides at 3′ seed region shown in *Italics*) and 3PS-2′-OMe-232425-crRNA$_{EMX1}$ containing AGAAGAAGAA*GUU*^{m*}*U*^{m*}*U*^{m*}) almost abolished the gene editing activity. The modified crRNA designs carrying other combinations of multiple PS-2′-OMe sites, including 3PS-2′-OMe-141718-crRNA$_{EMX1}$ (containing AGAA^{m*}GAA^{m*}G^{m*}AA), 3PS-2′-OMe-161820-crRNA$_{EMX1}$ (containing AGAAGA^{m*}AG^{m*}AA^{m*}), 3PS-2′-OMe-161718-crRNA$_{EMX1}$ (containing AGAAGA^{m*}A^{m*}G^{m*}AA), and 4PS-2′-OMe-14161820-crRNA$_{EMX1}$ (containing AGAA^{m*}GA^{m*}AG^{m*}AA^{m*}), preserved the gene-editing activity (Fig. S4†). Collectively, we chose to move forward with 3PS-2′-OMe-141718-crRNA$_{EMX1}$, which is the most active design.

We reacted 3PS-2′-OMe-141718-crRNA$_{EMX1}$ with BO-Br and CM-Br to obtain 3BO-141718-crRNA$_{EMX1}$ and 3CM-141718-crRNA$_{EMX1}$. The BO- and CM-containing crRNAs were converted
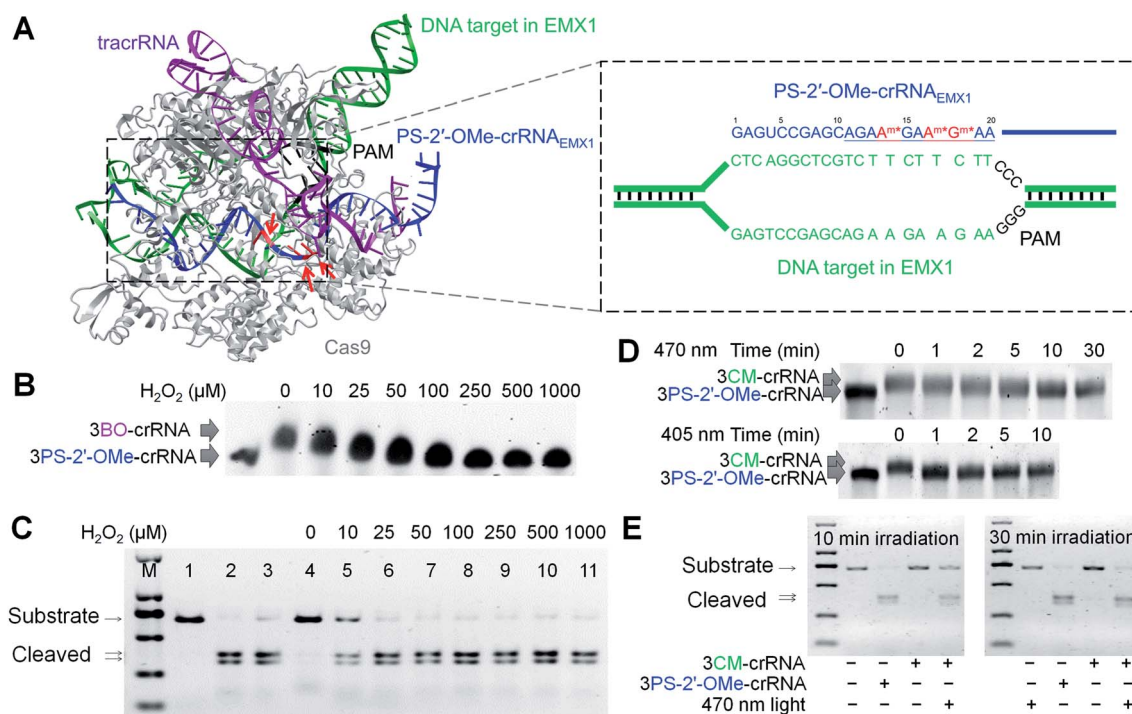

Fig. 2 Stimuli-responsive gRNA for conditional control of CRISPR-Cas9 function *in vitro*. (A) CRISPR-Cas9 complex containing Cas9 (gray), PS-2′-OMe-modified crRNA$_{EMX1}$ (blue) targeting the human EMX1 DNA, tracrRNA (purple), and substrate DNA (green) with a PAM (black). The red arrows and red nucleotides indicate PS-2′-OMe sites in crRNA$_{EMX1}$ used for BO and CM modifications. Inset is the unwound human EMX1 locus targeted by the PS-2′-OMe-crRNA$_{EMX1}$ containing 3 PS-2′-OMe sites. The 10-nt seed region is underlined. A^{m*} and G^{m*} in red are PS-2′-OMe-modified nucleotides. (B) Removal of BO from 3BO-141718-crRNA$_{EMX1}$ by H$_2$O$_2$ at different concentrations. Reactions were allowed to proceed for 1 h at 37 °C. (C) Cleavage of double-stranded EMX1 DNA substrate by unmodified and modified crRNAs with or without H$_2$O$_2$ treatment. From left to right: lane 1–3, DNA only, DNA + crRNA$_{EMX1}$, DNA + 3PS-2′-OMe-141718-crRNA$_{EMX1}$; lane 4–11, DNA + 3BO-141718-crRNA$_{EMX1}$ treated with H$_2$O$_2$ at indicated concentrations. "M" is the ladder lane containing DNA standards of 100, 250, 500, 750, 1000, and 2000 bp. Cas9 and tracrRNA were supplied in all the reactions. (D) Time-dependent removal of CM from 3CM-141718-crRNA$_{EMX1}$ when irradiated by visible light at 470 nm (top) or 405 nm (bottom). (E) Cleavage of double-stranded EMX1 DNA substrate promoted by 3PS-2′-OMe-141718-crRNA$_{EMX1}$ and 3CM-141718-crRNA$_{EMX1}$ with different duration of light irradiation. Cas9 and tracrRNA were supplied in all the reactions.

back to 3PS-2′-OMe-141718-crRNA$_{EMX1}$ *in vitro* by H$_2$O$_2$ treatment and visible light irradiation, respectively, as characterized by ESI-MS (Fig. S5†). Removal of BO by H$_2$O$_2$ and CM by visible light were again dose- and time-dependent (Fig. 2B and D), with similar kinetics shown previously with the 3BO- and 3CM-modified 20-nt model RNA (Fig. 1C and F). We found 3BO-141718-crRNA$_{EMX1}$ and 3CM-141718-crRNA$_{EMX1}$ were stable in the presence of biological nucleophiles such as lysine and glutathione at a concentration of 5 mM at 37 °C, indicating the modified crRNA strands are stable against them under physiological conditions (Fig. S6†). As illustrated in Fig. 2C, in the presence of tracrRNA and Cas9, 3PS-2′-OMe-141718-crRNA$_{EMX1}$ facilitated full cleavage of the substrate DNA *in vitro* at 37 °C in 1 h. The comparable activity of 3PS-2′-OMe-141718-crRNA$_{EMX1}$ with the native crRNA$_{EMX1}$ suggests that the three PS-2′-OMe modifications in crRNA$_{EMX1}$ did not interfere with the DNA-cleaving activity. In contrast, as a result of the perturbing effects of the BO and CM modifications, 3BO-141718-crRNA$_{EMX1}$ and 3CM-141718-crRNA$_{EMX1}$ were inactive and no DNA cleavage

was observed under the same condition (Fig. 2C and E), indicating BO- and CM-modified crRNAs had little basal activities in the absence of stimuli. Partial activation of 3BO-141718-crRNA$_{EMX1}$ was observed when supplying H$_2$O$_2$ at a concentration of 10 μM. The corresponding cleavage reaction showed a decreased efficiency compared to 3PS-2′-OMe-141718-crRNA$_{EMX1}$ due to incomplete removal of BO. Full activity restoration of 3BO-141718-crRNA$_{EMX1}$ was achieved when the concentration of H$_2$O$_2$ was increased to 25 μM and above (Fig. 2C). Activation of 3CM-141718-crRNA$_{EMX1}$ *in vitro* by visible light was also achieved when irradiated for 10 min at 470 nm and 1 min at 405 nm (Fig. 2D and E).

2.3. Stimuli-responsive gRNA for conditional control of CRISPR-Cas9-mediated EMX1 gene editing in human cells

Encouraged by the above results, we applied these rosa-crRNA and vila-crRNA for controllable gene editing in Cas9-expressing human embryonic kidney 293T (HEK293T-Cas9) cells (Fig. 3). The modified crRNAs were introduced along
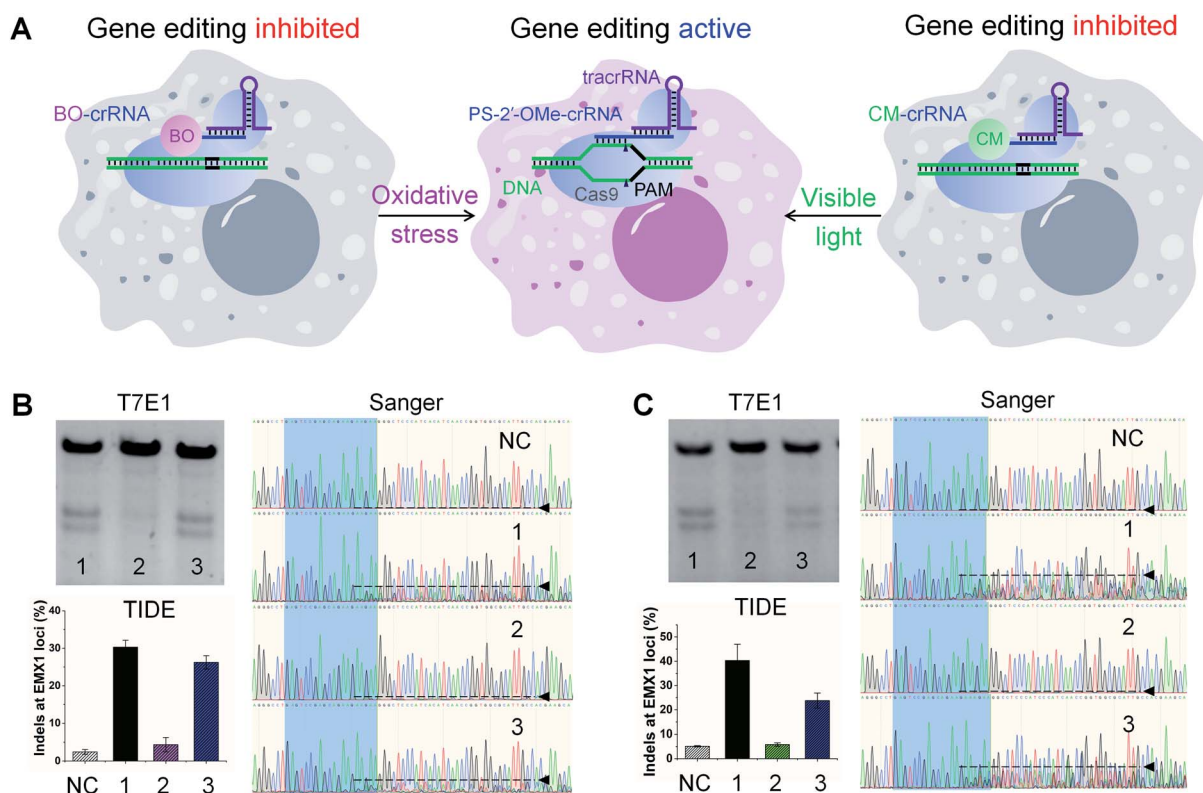

Fig. 3 Stimuli-responsive gRNA for conditional control of CRISPR-Cas9-mediated EMX1 gene editing in human embryonic kidney 293T cells. (A) Schematic of using BO- and CM-modified crRNA along with tracrRNA and Cas9 for ROS- and visible light-controlled editing of EMX1 gene in human cells, respectively. (B) Oxidative stress-controlled gene editing enabled by 3BO-141718-crRNA$_{EMX1}$. T7E1 and TIDE assays: indel formation at the EMX1 loci of HEK293T-Cas9 cells promoted by 3PS-2′-OMe-141718-crRNA$_{EMX1}$ (lane 1) and 3BO-141718-crRNA$_{EMX1}$ treated without (lane 2) or with (lane 3) oxidative stress, where "NC" indicates the negative control sample with no crRNA. Error bars are from cell samples in three separated wells. Sanger chromatograms: exemplary Sanger sequencing results used for the TIDE calculation, where the dash lines and arrows indicate the level of disturbance as a visualization of indel formation. The crRNA-targeting sequence region in sequencing results is highlighted in blue. TracrRNA was cotransfected with the crRNA strands for all the samples. (C) Visible light-sensitive gene editing facilitated by 3CM-141718-crRNA$_{EMX1}$. T7E1 and TIDE assays: indel formation at the EMX1 loci of HEK293T-Cas9 cells promoted by 3PS-2′-OMe-141718-crRNA$_{EMX1}$ (lane 1) and 3CM-141718-crRNA$_{EMX1}$ in dark (lane 2) or irradiated by visible light at 470 nm (lane 3). "NC" indicates the negative control sample with no crRNA. Error bars are from cell samples in three separated wells. Sanger chromatograms are labeled similarly as in (B). TracrRNA was cotransfected with the crRNA strands for all the samples.

with the tracrRNA into the cells through lipid-mediated transfection. If the crRNA is active, double-stranded breaks will be generated in the genome at the EMX1 loci, which can be repaired through the non-homologous end-joining pathway to result in random insertions and deletions (indels). We measured the frequencies of indel formation using two assays: T7 endonuclease I (T7E1) assay[77] based on PAGE, and tracking of indels by decomposition (TIDE) assay[78] based on Sanger sequencing.

To test ROS-responsive gene editing (Fig. 3A), oxidative stress was induced in cells by supplying 100 μM H_2O_2 to the culture media for 10 min before transfection.[79,80] We used 3PS-2′-OMe-141718-crRNA$_{EMX1}$ as a positive control and detected strong editing by both T7E1 and TIDE assays, with an indel frequency of 30.3% reported by TIDE (Fig. 3B). The oxidative stress itself was found to induce neither background indels in the absence of crRNA nor any additional editing in the presence of crRNA (Fig. S7†). We found that in our hands, T7E1 and TIDE assays were generally in good agreement and all the quantitative indel frequencies reported in the following are therefore based on TIDE. In cells transfected with 3BO-141718-crRNA$_{EMX1}$ (containing AGAA^{BO}GAA^{BO}G^{BO}AA , BO-modified phosphorothioate as superscripted BO), a very low editing rate of 4.4% was detected in the absence of oxidative stress due to the blocking effect of BO modifications. An indel frequency of 2.4% was detected in cells that were not transfected with any crRNA as the negative control (Fig. 3B). We suspect that this 2.4% indel rate was a result of the intrinsic noise associated with the TIDE calculation by comparing Sanger sequencing data from cells in different wells,[81] because the sequencing chromatogram of the negative control is clean and with almost no disturbance caused by indels (Fig. 3B). We attributed the low-level editing promoted by 3BO-141718-crRNA$_{EMX1}$, as 2.0% after subtracting 2.4% from 4.4%, to its weak background activity under intracellular environment that was different from in vitro, though almost no background activity was observed in the in vitro assay shown previously in Fig. 2C. In contrast to this low rate, the gene-editing activity of 3BO-141718-crRNA$_{EMX1}$ was successfully triggered by oxidative stress to reach an indel frequency of 26.2% (Fig. 3B), corresponding to a 6.0-fold activation (12-fold net activation when subtracting noise reported by the negative control). The exemplary Sanger sequencing chromatograms, which were among those used for the TIDE calculation, are shown for a better visualization of the degree of indel formation (Fig. 3B).

Three BO modifications were found essential for the high level of activity enhancement by minimizing background activities. Using 1BO-18-crRNA$_{EMX1}$ (containing AGAA-GAAG^{BO}AA) and 2BO-1718-crRNA$_{EMX1}$ (containing AGAAGAA-^{BO}G^{BO}AA) we could only achieve 1.6-fold and 2.4-fold activation under the same stimulation condition, respectively, owing to elevated basal level activities because of less effective blocking (Fig. S8a†). Activation of gene editing by oxidative stress was also successfully achieved using 3BO-161820-crRNA$_{EMX1}$ (containing AGAAGA^{BO}AG^{BO}AA^{BO} 4.0-fold), 3BO-161718-crRNA$_{EMX1}$ (containing AGAAGA^{BO}A^{BO}G^{BO}AA 5.4-fold) and 4BO-14161820-crRNA$_{EMX1}$ (containing AGAA^{BO}GA^{BO}AG^{BO}AA^{BO} 5.9-fold),

suggesting the strategy of BO modifications at different PS-2′-OMe sites is generally applicable for constructing rosa-crRNA (Fig. S9†), as long as the PS-2′-OMe sites are innocent for the gene-editing activity. We expect that background activity could be further reduced if more BO modifications are introduced at proper sites in the crRNA as well as the tracrRNA.

To enable visible light-activated gene editing, cells transfected with 3CM-141718-crRNA$_{EMX1}$ (containing AGAA^{CM}GAA^{CM}G^{CM}AA, CM-modified phosphorothioate as superscripted CM) and tracrRNA were irradiated with or without 470 nm light and assayed for indel formation (Fig. 3C). The HEK293T-Cas9 cells carrying 3CM-141718-crRNA$_{EMX1}$ and tracrRNA that were grown in dark conferred an indel rate of 5.8% (Fig. 3C), whereas cells that were not transfected with any crRNA reported 5.1% editing as a negative control under the same assay condition. Again, as indel formation should not be initiated in cells carrying no crRNA, we suspect the observed 5.1% editing was a result of the intrinsic noise of TIDE calculation from cells in different wells,[81] because the Sanger sequencing chromatogram of the negative control is clean with almost no disturbance (Fig. 3C). In cells carrying 3CM-141718-crRNA$_{EMX1}$ and tracrRNA that were treated with visible light for 10 min, a much higher indel rate of 23.8% was detected (Fig. 3C), corresponding to a 4.1-fold activation (27-fold net activation when subtracting noise reported by the negative control). The positive control 3PS-2′-OMe-crRNA$_{EMX1}$ introduced an indel frequency of 40.3% under the same assay condition (Fig. 3C). Similar to BO-modified crRNA, three CM modifications were required to achieve efficient light activation, with 1CM-18-crRNA$_{EMX1}$ (containing AGAAGAAG^{CM}AA) and 2CM-1718-crRNA$_{EMX1}$ (containing AGAAGAA^{CM}G^{CM}AA) conferring only 1.4-fold and 1.6-fold activation, respectively (Fig. S8b†).

2.4. Stimuli-responsive gRNA for ROS-controlled editing of HBB gene with Cas9 mRNA delivery

We next switched to another genomic locus, HBB, to test if our rosa-crRNA strategy could also be applied to crRNA containing a different spacer sequence. We simultaneously assayed for compatibility of chemically modified crRNAs with mRNA delivery of Cas9 using HEK293T cells.[7,8] Learning directly from the success of 3BO-141718-crRNA$_{EMX1}$, we chose to introduce BO modifications at $G_{14}G_{17}U_{18}$ in the seed region of the 42-nt crRNA$_{HBB}$ (Fig. 4A) to obtain 3BO-141718-crRNA$_{HBB}$ (containing the seed region of AGGG^{BO}CAG^{BO}U^{BO}AA). Indeed, 3PS-2′-OMe-141718-crRNA$_{HBB}$, among several variants with different modification sites, showed comparable activity with the native crRNA$_{HBB}$ (Fig. S10†). Successful BO incorporation to afford 3BO-141718-crRNA$_{HBB}$ was confirmed by PAGE (Fig. 4B) and ESI-MS (Fig. S11†) analyses. H_2O_2 promoted conversion of 3BO-141718-crRNA$_{HBB}$ back to 3PS-2′-OMe-141718-crRNA$_{HBB}$ (Fig. 4B) with very similar kinetics as 3BO-141718-crRNA$_{EMX1}$ (Fig. 2B). H_2O_2-activated DNA targeting by 3BO-141718-crRNA$_{HBB}$ was also observed in vitro (Fig. 4C). In HEK293T cells pre-transfected with the tracrRNA and the mRNA encoding Cas9,[82,83] efficient editing was introduced by 3PS-2′-OMe-141718-crRNA$_{HBB}$ at the HBB loci with an indel frequency of 36.2%, confirming that chemically modified crRNA is
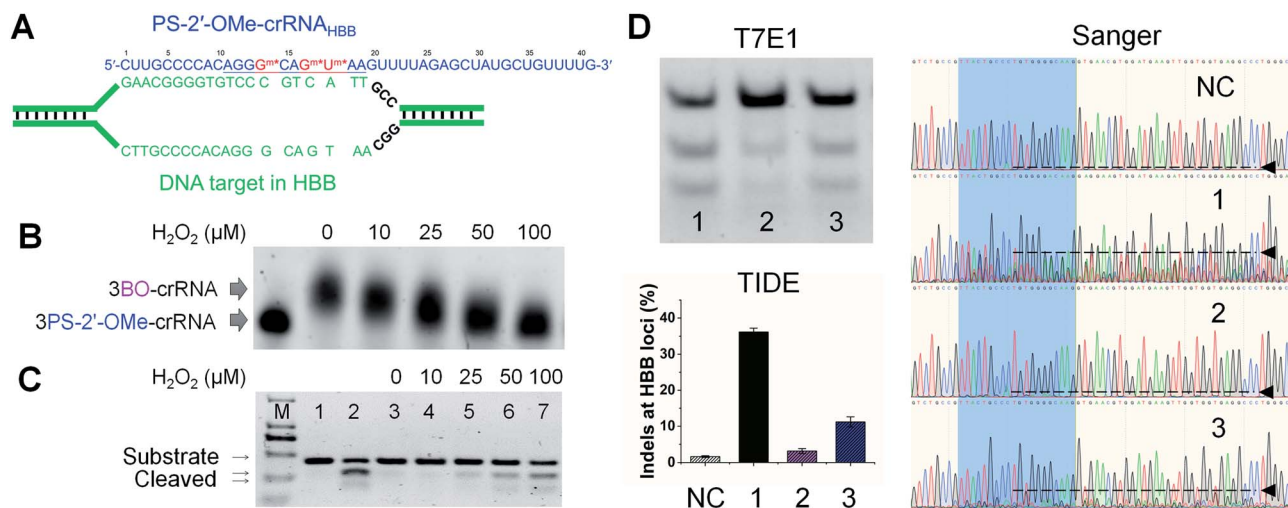
Fig. 4 Conditional control of CRISPR-Cas9-mediated HBB gene editing in human embryonic kidney 293T cells using stimuli-responsive gRNA and Cas9 mRNA delivery. (A) Unwound HBB locus targeted by 3PS-2′-OMe-141718-crRNA$_{HBB}$ generated through decaging 3BO-141718-crRNA$_{HBB}$ by H$_2$O$_2$. The seed region is underlined. G^{m*} and U^{m*} in red are PS-2′-OMe-modified nucleotides. (B) Removal of BO from 3BO-141718-crRNA$_{HBB}$ in the presence of H$_2$O$_2$ at different concentrations. Reactions were allowed to proceed for 1 h at 37 °C. (C) Cleavage of double-stranded HBB DNA substrate by crRNA$_{HBB}$ variants in the presence of tracrRNA and Cas9 in vitro. From left to right: lane 1–2, DNA only, DNA + 3PS-2′-OMe-141718-crRNA$_{HBB}$; lane 3–7, DNA + 3BO-141718-crRNA$_{HBB}$ treated with H$_2$O$_2$ at indicated concentrations. "M" is the ladder lane containing DNA standards of 100, 250, 500, 750, 1000, and 2000 bp. (D) T7E1 and TIDE assays: indel formation at the HBB loci of HEK293T cells promoted by 3PS-2′-OMe-141718-crRNA$_{HBB}$ (lane 1) and 3BO-141718-crRNA$_{HBB}$ treated without (lane 2) or with (lane3) H$_2$O$_2$. "NC" is the control sample with no crRNA. Error bars are from cell samples in three separated wells. Sanger chromatograms are labeled similarly as in Fig. 3B. Cas9 mRNA and tracrRNA were cotransfected with the crRNA strands.

compatible with Cas9 mRNA delivery (Fig. 4D). Strong activity inhibition by BO was observed for 3BO-141718-crRNA$_{HBB}$, which conferred an indel rate of 3.1% in cells without oxidative stress (Fig. 4D). An indel frequency of 1.6% was detected in cells that did not contain any crRNA as a negative control. A 3.6-fold activation was achieved by 3BO-141718-crRNA$_{HBB}$ stimulated by oxidative stress, reaching an indel rate of 11.2% (Fig. 4D). This indel rate corresponds to an activation ratio of 6.4 after background subtraction. The lower activity of decaged 3BO-141718-crRNA$_{HBB}$ compared to 3PS-2′-OMe-141718-crRNA$_{HBB}$ was observed likely due to staggered peak activities of the decaged crRNA and the transiently expressed Cas9 mRNA. Nevertheless, a 3.6-fold activation was readily distinguishable when cells experienced oxidative stress, and the efficiency could be further improved using other delivery strategies to ensure a more persistently active window for both Cas9 and tracrRNA inside cells.[5,7]

PS-2′-OMe modifications on gRNA were reported to maintain or reduce off-target effects of the Cas9/gRNA complex.[11,12] We analyzed two major off-target sites of EMX1 in the human genome and found the native crRNA$_{EMX1}$ showed significant indel formation at off-target site 1 because of the strong sequence similarity (Table S1 and Fig. S12†). In contrast, indel formation at two off-target sites was below our detection limit for 3PS-2′-OMe-141718-crRNA$_{EMX1}$, which is the fully activated form of the BO- and CM-modified crRNA$_{EMX1}$. As BO and CM modifications offer an additional layer of activity control to limit the exposure of cells to gene-editing agents, we conclude that the specificity of rosa-crRNA and vila-crRNA should be at

least as good as that of PS-2′-OMe-modified crRNA and could be better than that of unmodified crRNA.

CRISPR tools utilize very similar principles of nucleic acid substrate recognition by base-paring with gRNA, so that the strategy reported in this work for gRNA modification based on phosphorothioate chemistry should be also applicable in cases beyond traditional Cas9-mediated gene editing, such as those for stimuli-responsive CRISPR interference/activation,[84,85] DNA base editing[86] and RNA editing.[87] In addition, antisense oligonucleotides containing DNA phosphorothioates with controlled stereochemistry were obtained by solid-phase synthesis[88,89] and showed much higher efficacy in silencing gene expressions than the racemic mixtures.[90] Although there is currently no method reported for solid-phase synthesis of RNA oligonucleotides containing multiple phosphorothioates with defined stereochemistry, we expect that using gRNA with chirally controlled PS-2′-OMe modifications to construct stimuli-responsive CRISPR tools would result in significantly improved performance.

3. Conclusions

In summary, we developed a general method for preparing stimuli-responsive RNA through site-specific derivatization of PS-2′-OMe. We successfully modified RNA oligonucleotides with ROS- and visible light-labile groups that were challenging to incorporate by other methods. The rosa-RNA and vila-RNA prepared by this strategy showed robust activation in the presence of ROS and visible light, respectively. We further tested the rosa-RNA and vila-RNA architecture in crRNA and successfully

demonstrated ROS- and visible light-controlled gene editing in human HEK293T cells mediated by CRISPR-Cas9. Because PS-2′-OMe-modified RNAs are commercially available at low cost and the reaction between PS-2′-OMe and arylmethylbromides can be readily expanded to a wide variety of aryl groups, our method can be generalized to introduce many other functional groups into gRNA site-specifically. With a method for facile preparation based on PS-2′-OMe that is already used in many FDA-approved oligonucleotide drugs such as antisense DNA and siRNA, we expect chemically modified gRNA to be more widely adapted by researchers to facilitate precise gene editing and regulation in live cells, as well as actively studied as candidates for gene therapies.

4. Experimental Section

4.1. Materials

Chemicals for buffer preparation and synthesis, including 4-bromomethylphenylboronic acid pinacol ester and 4-hydroxymethyl-7-diethylaminocoumarin were from either Sigma Aldrich (Shanghai, China), Alfa Aesar (Tianjin, China) or Tokyo Chemical Industry (TCI) Development (Shanghai, China). Hydrogen peroxide solutions used in this study was diluted from 30% w/w water stock solution from Sigma Aldrich. Enzymes including Q5® high-fidelity DNA polymerase for PCR amplification and T7 endonuclease I for indels assays were from New England BioLabs (Beijing, China). TrueGuide™ tracrRNA, Cas9 mRNA, and Lipofectamine® RNAiMAX were from Thermo Fisher Scientific (Shanghai, China). Dulbecco's modified Eagle's medium (DMEM), Dulbecco's phosphate buffered saline (DPBS), Opti-MEM medium, fetal bovine serum (FBS), 100 IU per mL penicillin-streptomycin and 0.25% trypsin were purchased from Corning Cellgro (NY, USA). HEK293T-Cas9 cells were purchased from GeneCopoeia (MD, USA). HEK293T cells were from were from National Platform of Experimental Cell Resources for Sci-Tech (Beijing, China). Oligonucleotides were synthesized and purified by either Integrated DNA Technologies (IA, USA), Genscript (Jiangsu, China) or Hippobio (Zhejiang, China). Lucigen QuickExtract™ DNA extraction solution was from Lucigen (WI, USA).

List of RNA oligonucleotides used in this work from 5′ to 3′:

(1) 20-nt RNA: GAGUCCGAGCAGAAGAAGAA.

(2) 20-nt 1PS-RNA: GAGUCCGAGC*AGAAGAAGAA.

(3) 20-nt 1PS-2′-OMe-RNA: GAGUCCGAGC^{m}AGAAGAAGAA.

(4) 20-nt 3PS-RNA: GAGUCCGAGC*A*G*AAGAAGAA.

(5) 20-nt 3PS-2′-OMe-RNA: GAGUCCGAGC^{m*}A^{m*}G^{m*}AAGAAGAA.

(6) crRNA$_{EMX1}$:

GAGUCCGAGCAGAAGAAGAAGUUUUAGAGCUAUGCUGUUUUG.

(7) 1PS-2′-OMe-18-crRNA$_{EMX1}$:

GAGUCCGAGCAGAAGAAG^{m*}AAGUUUUAGAGCUAUGCUGUUUUG.

(8) 2PS-2′-OMe-1718-crRNA$_{EMX1}$:

GAGUCCGAGCAGAAGAA^{m*}G^{m*}AAGUUUUAGAGCUAUGCUGUUUUG.

(9) 3PS-2′-OMe-141718-crRNA$_{EMX1}$:

GAGUCCGAGCAGAA^{m*}GAA^{m*}G^{m*}AAGUUUUAGAGCUAUGCUGUUUUG.

(10) 3PS-2′-OMe-161820-crRNA$_{EMX1}$:

GAGUCCGAGCAGAAGA^{m*}AG^{m*}AA^{m*}GUUUUAGAGCUAUGCUGUUUUG

(11) 3PS-2′-OMe-161718-crRNA$_{EMX1}$:

GAGUCCGAGCAGAAGA^{m*}A^{m*}G^{m*}AAGUUUUAGAGCUAUGCUGUUUUG.

(12) 3PS-2′-OMe-171819-crRNA$_{EMX1}$:

GAGUCCGAGCAGAAGAA^{m*}G^{m*}A^{m*}AGUUUUAGAGCUAUGCUGUUUUG.

(13) 4PS-2′-OMe-14161820-crRNA$_{EMX1}$:

GAGUCCGAGCAGAA^{m*}GA^{m*}AG^{m*}AA^{m*}GUUUUAGAGCUAUGCUGUUUUG.

(14) 3PS-2′-OMe-212223-crRNA$_{EMX1}$:

GAGUCCGAGCAGAAGAAGAAG^{m*}U^{m*}U^{m*}UUAGAGCUAUGCUGUUUUG.

(15) 3PS-2′-OMe-232425-crRNA$_{EMX1}$:

GAGUCCGAGCAGAAGAAGAAGUU^{m*}U^{m*}U^{m*}AGAGCUAUGCUGUUUUG.

(16) crRNA$_{HBB}$:

CUUGCCCCACAGGGCAGUAAGUUUUAGAGCUAUGCUGUUUUG.

(17) 2PS-2′-OMe-1718-crRNA$_{HBB}$:

CUUGCCCCACAGGGCAG^{m*}U^{m*}AAGUUUUAGAGCUAUGCUGUUUUG.

(18) 3PS-2′-OMe-141718-crRNA$_{HBB}$:

CUUGCCCCACAGGG^{m*}CAG^{m*}U^{m*}AAGUUUUAGAGCUAUGCUGUUUUG.

(19) 3PS-2′-OMe-161820-crRNA$_{HBB}$:

CUUGCCCCACAGGGCA^{m*}GU^{m*}AA^{m*}GUUUUAGAGCUAUGCUGUUUUG.

(20) 4PS-2′-OMe-14161820-crRNA$_{HBB}$:

CUUGCCCCACAGGG^{m*}CA^{m*}GU^{m*}AA^{m*}GUUUUAGAGCUAUGCUGUUUUG.

(21) 4PS-2′-OMe-14171820-crRNA$_{HBB}$:

CUUGCCCCACAGGG^{m*}CAG^{m*}U^{m*}AA^{m*}GUUUUAGAGCUAUGCUGUUUUG.

(22) tracrRNA:

GGAACCAUUCAAAACAGCAUAGCAAGUUAAAAUAAGGCUAGUCCGUUAUCAACUUGAAAAAGUGGCACCGAGUCGGUGCUUU.

In the above sequences, "N*" and "N^{m*}" represent PS-2′-OH and PS-2′-OMe modifications, respectively. Underlined are the seed regions of crRNAs. *Italic* are the hybridizing regions between crRNAs and the tracrRNA. The tracrRNA used in this study is a commercial product from Thermo Fisher Scientific that may contain some undisclosed chemical modifications for performance improvement.

4.2. Synthesis of 4-bromomethyl-7-diethylaminocoumarin

A batch of 0.25 g 4-hydroxymethyl-7-diethylaminocoumarin was dissolved in 25 mL dichloromethane, to which 0.5 mL phosphorus tribromide was dropwise added at room temperature. After stirring for 0.5 h, water was added to the mixture above to quench the reaction. The reaction mixture was extracted with dichloromethane/water. The organic layer was dried with

Na$_2$SO$_4$, filtered and evaporated to obtain CM-Br at almost quantitative yield. ^{1}H-NMR (300 MHz, CDCl$_3$), δ (ppm): 7.50 (d, 1H), 6.64 (d, 1H), 6.51 (s, 1H), 4.4 (s, 2H), 3.4 (q, 4H), 1.2 (t, 6H). ^{13}C-NMR (300 MHz, CDCl$_3$), δ (ppm): 161.79, 156.76, 150.91, 150.36, 125.42, 115.41, 109.30, 108.70, 106.20, 97.91, 44.84, 27.17, 12.49. LCMS-IT-TOF spectrometry: calc. for C$_{14}$H$_{16}$BrNO$_2$, [M + H]$^+$ 310.0, found 310.0. See Fig. S12† for the NMR spectra.

4.3. Synthesis of BO-modified RNA and CM-modified RNA

BO-modified RNA and CM-modified RNA were prepared by reacting BO-Br and CM-Br with RNA containing PS-2′-OMe modifications, respectively. To a 20 µL solution of 50 µM RNA in 50 mM sodium phosphate buffer at pH 6.0 was added 20 µL 25 mM BO-Br or CM-Br in DMF. The solution was kept on a roller at room temperature for 48 h. The resulting solution was purified by Amicon-10K ultrafilters using water to remove excess BO-Br or CM-Br and desalted for 8 times. The concentration of the modified RNA solution was quantified by the standard UV260 method, and the stock solution was diluted for desired concentrations. Denatured PAGE and ESI-MS were used to characterize the modified RNA products. ESI-MS measurement was either provided by Hippobio (Zhejiang, China), Sango Biotech (Shanghai, China) or performed on a Thermo Scientific LTQ XL™ Linear Ion Trap MS at Tsinghua University. Upon storage at −20 °C, BO-RNA and CM-RNA were found stable in stock solution for at least 6 months.

4.4. PAGE analysis of RNAs

For H$_2$O$_2$-incuded removal of BO modifications, to a solution of 1 µM BO-RNA in NEBuffer™ 3.1 buffer (20 mM HEPES, 100 mM NaCl, 5 mM MgCl$_2$, 0.1 mM EDTA, pH 6.5) was added H$_2$O$_2$ with desired concentration (0–1 mM). The solution was incubated in a PCR machine (Thermo Fisher Scientific Proflex PCR system) at 37 °C for a desired time (0–20 h). For visible light-induced removal of CM modifications, a solution of 1 µM CM-RNA in NEBuffer™ 3.1 buffer was kept in a cell incubator installed with 3 W LED bulbs which can emit blue light (405 nm or 470 nm). The LED bulb was powered by an adjustable DC regulated power supply, reaching the CM-RNA solution or cells at 13 mW cm^{-2} for 0–30 min. Powers of light irradiations at samples were measured by a PM100D digital optical power and energy meter purchased from Thorlabs GmbH.

For PAGE analysis, 5 pmol RNA samples were mixed with an equivalent volume of a loading buffer containing 8 M urea, 0.03% bromophenol blue and 0.03% xylene cyanol FF, and then electrophoresed at 200 V for about 1.5 h on 15% denatured poly-acrylamide gels (29 : 1 monomer to bis ratio, 8 M urea) in 1× MOPS running buffer (40 mM MOPS, pH 7.0, 10 mM sodium acetate, 1 mM EDTA) using the vertical electrophoretic apparatus (DYY-6C, Liuyi Instrument Factory, Beijing, China). After 1× SYBR™ Gold (Thermo Fisher Scientific) staining, the gels were visualized using a Biorad Gel Doc XR+ Gel Documentation System. We found the commonly used tris-borate-EDTA (TBE) buffer for PAGE analysis was not suitable for BO-modified RNA, possibly because of the strong interaction between boronate and tris that contains multiple proximate hydroxyl groups. For PAGE analysis of

RNAs other than BO-RNA, 1× TBE running buffer (90 mM Tris, 90 mM boric acid, 1 mM EDTA, pH 8.3) could be used.

4.5. ROS-activated and visible light-activated crRNAs for CRISPR-Cas9 activity *in vitro*

In vitro DNA cutting assay was adapted from the protocol provided by NEB (protocol M0386). EMX1 fw and EMX1 rv (Table S1, ESI†) were used as the primers for EMX1 dsDNA substrate preparation, with genomic DNA from 293T-Cas9 cells (Lucigen QuickExtract™ for DNA extraction) as the template. To a combined solution of 2.5 µL 10 µM EMX1 fw, 2.5 µL 10 µM EMX1 rv, 19.5 µL H$_2$O and 0.5 µL genomic DNA was added to 25 µL 2× Q5 Master Mix (NEB) and then the PCR protocol following the Q5® high-fidelity DNA polymerase guideline was applied. The PCR products were purified using a Gel Extraction Kit (Omega) following the manufacturer's protocol. The purified PCR products were used as the dsDNA substrates for *in vitro* CRISPR-Cas9 cleavage assay.

For ROS activation, to a combined solution of 1 µL 1 µM crRNA w/wo BO modifications, 1 µL 1 µM tracrRNA, 0.5 µL 1 µM Cas9, 1 µL H$_2$O$_2$ stock solutions at desired concentrations, 1 µL 30 nM dsDNA substrate and 24.5 µL H$_2$O was mixed with 1 µL 10× NEBuffer™ 3.1 buffer in a PCR tube and incubated at 37 °C for 1 h in the PCR machine. The reaction product was then mixed with 1/6 volume of 6× loading buffer and loaded on a 1.5% agarose gel containing 1× GelRed (Sigma Aldrich) and running at 160 V in 1× TBE buffer for around 30 min. The gels were visualized using a Biorad Gel Doc XR+ Gel Documentation System.

For visible light activation, the procedures were as above except for the use of light irradiation (405 nm or 470 nm) at 13 mW cm^{-2} for 0–30 min and the lack of H$_2$O$_2$.

4.6. ROS-activated and visible light-activated crRNAs for CRISPR-Cas9-mediated gene editing of EMX1 in HEK293T-Cas9 cells

HEK293T-Cas9 cells (GeneCopoeia) stably expressing Cas9 protein were cultured in 48-well plates (∼40 000 cells seeded per well) in DMEM plus GlutaMAX (Life Technologies) with 10% FBS. The cells were ready for transfection after about 20 h when reaching ∼70% confluence.

For ROS-activation, to induce oxidative stress of the cells, H$_2$O$_2$ was added to the culture medium to a final concentration of 100 µM for 10 min before immediately changing to the following transfection medium. Transfection was performed using 20 pmol crRNA$_{EMX1}$ (w/wo chemical modifications), 20 pmol tracrRNA and 1 µL RNAiMAX reagent (Life Technologies) according to the manufacturer's protocol to target the EMX1 locus of the 293T-Cas9 cells. Cells were harvested 2 days after transfection. The harvested cells were rinsed with DPBS (Life Technologies) for 3 times and then suspended in 200 µL Lucigen QuickExtract™ DNA extraction solution for quick genome DNA extraction as guided by the manufacturer's protocol. T7E1 and TIDE assays were used to evaluate indels as gene editing efficiency in the cells. The Sanger (first generation) sequencing for TIDE assays was performed by TsingKe Biological

Technology (Beijing, China). Off-target effects were evaluated using the same protocol except for the use of corresponding primers for PCR amplification to prepare the samples for T7E1 and TIDE assays.

For visible light activation, 20 pmol EMX1 crRNA$_{EMX1}$ (w/wo chemical modifications) and 20 pmol tracrRNA were transfected in each well using 1 µl RNAiMAX Reagent (Life Technologies) following the manufacturer's protocol to target the EMX1 locus of the 293T-Cas9 cells. After the gRNAs (crRNA and tracrRNA) were transfected, visible light irradiation (470 nm) was applied to the cells at 13 mW cm^{-2} for 10 min. The cells were harvested 2 days after transfection. The DNA extraction and T7E1 and TIDE assays were the same as above.

4.7. ROS-activated crRNAs for CRISPR-Cas9-mediated gene editing of HBB in HEK293T cells with Cas9 mRNA

HEK293T cells were cultured in 48-well plates ($\sim$40 000 cells seeded per well) in DMEM plus GlutaMAX (Life Technologies) with 10% FBS. The cells were first transfected with Cas9 mRNA after about 20 h when cells reached $\sim$70% confluence. The mRNA transfection used 125 ng Cas9 mRNA (Thermo Fisher Scientific) and 1 µL Lipofectamine™ MessengerMAX™ reagent (Life Technologies) for each well as suggested by the manufacturer's protocol. The cells were then incubated for 4 h to allow sufficient Cas9 protein translation. To induce oxidative stress of cells, H_2O_2 was added to the culture medium to a final concentration of 100 µM for 10 min before immediately changing to the gRNA transfection recopies. Transfection was performed using 30 pmol crRNA$_{HBB}$ (w/wo chemical modifications), 30 pmol tracrRNA and 1 µL RNAiMAX reagent (Life Technologies) according to the manufacturer's protocol to initiate editing in HBB locus of the HEK293T cells. Cells were harvested 2 days after transfection. The DNA extraction and T7E1 and TIDE assays were the same as above.

Author contributions

The paper was written through contributions of all authors. Chunmei Gu, Lu Xiao and Yu Xiang designed the study. Chunmei Gu, Lu Xiao and Xiao Xu performed the synthesis and *in vitro* characterization. Chunmei Gu, Jiachen Shang and Luo He performed the cellular experiment. All authors have given approval to the final version of the paper.

Conflicts of interest

There are no conflicts to declare.

Acknowledgements

Notes and references

1 R. Barrangou and J. A. Doudna, *Nat. Biotechnol.*, 2016, **34**, 933–941.

2 L. Cong, F. A. Ran, D. Cox, S. Lin, R. Barretto, N. Habib, P. D. Hsu, X. Wu, W. Jiang, L. A. Marraffini and F. Zhang, *Science*, 2013, **339**, 819–823.

3 P. Mali, L. Yang, K. M. Esvelt, J. Aach, M. Guell, J. E. DiCarlo, J. E. Norville and G. M. Church, *Science*, 2013, **339**, 823–826.

4 M. Jinek, A. East, A. Cheng, S. Lin, E. Ma and J. Doudna, *Elife*, 2013, **2**, e00471.

5 H. Yin, K. J. Kauffman and D. G. Anderson, *Nat. Rev. Drug Discovery*, 2017, **16**, 387–399.

6 D. Wilbie, J. Walther and E. Mastrobattista, *Acc. Chem. Res.*, 2019, **52**, 1555–1564.

7 H. X. Wang, M. Li, C. M. Lee, S. Chakraborty, H. W. Kim, G. Bao and K. W. Leong, *Chem. Rev.*, 2017, **117**, 9874–9906.

8 A. S. Piotrowski-Daspit, P. M. Glaze and W. M. Saltzman, *Curr. Opin. Biomed. Eng.*, 2018, **7**, 24–32.

9 C. A. Vakulskas, D. P. Dever, G. R. Rettig, R. Turk, A. M. Jacobi, M. A. Collingwood, N. M. Bode, M. S. McNeill, S. Q. Yan, J. Camarena, C. M. Lee, S. H. Parka, V. Wiebking, R. O. Bak, N. Gomez-Ospina, M. Pavel-Dinu, W. C. Sun, G. Bao, M. H. Porteus and M. A. Behlke, *Nat. Med.*, 2018, **24**, 1216–1224.

10 D. Rosenblum, A. Gutkin, R. Kedmi, S. Ramishetti, N. Veiga, A. M. Jacobi, M. S. Schubert, D. Friedmann-Morvinski, Z. R. Cohen, M. A. Behlke, J. Lieberman and D. Peer, *Sci. Adv.*, 2020, **6**, eabc9450.

11 A. Hendel, R. O. Bak, J. T. Clark, A. B. Kennedy, D. E. Ryan, S. Roy, I. Steinfeld, B. D. Lunstad, R. J. Kaiser, A. B. Wilkens, R. Bacchetta, A. Tsalenko, D. Dellinger, L. Bruhn and M. H. Porteus, *Nat. Biotechnol.*, 2015, **33**, 985–989.

12 M. Rahdar, M. A. McMahon, T. P. Prakash, E. E. Swayze, C. F. Bennett and D. W. Cleveland, *Proc. Natl. Acad. Sci. U. S. A.*, 2015, **112**, E7110–E7117.

13 K. Lee, V. A. Mackley, A. Rao, A. T. Chong, M. A. Dewitt, J. E. Corn and N. Murthy, *Elife*, 2017, **6**, e25312.

14 H. Yin, C. Q. Song, S. Suresh, Q. Wu, S. Walsh, L. H. Rhym, E. Mintzer, M. F. Bolukbasi, L. J. Zhu, K. Kauffman, H. Mou, A. Oberholzer, J. Ding, S. Y. Kwan, R. L. Bogorad, T. Zatsepin, V. Koteliansky, S. A. Wolfe, W. Xue, R. Langer and D. G. Anderson, *Nat. Biotechnol.*, 2017, **35**, 1179–1187.

15 H. Yin, C. Q. Song, S. Suresh, S. Y. Kwan, Q. Wu, S. Walsh, J. Ding, R. L. Bogorad, L. J. Zhu, S. A. Wolfe, V. Koteliansky, W. Xue, R. Langer and D. G. Anderson, *Nat. Chem. Biol.*, 2018, **14**, 311–316.

16 A. Deiters, *Curr. Opin. Chem. Biol.*, 2009, **13**, 678–686.

17 Q. Y. Liu and A. Deiters, *Acc. Chem. Res.*, 2014, **47**, 45–55.

18 S. G. Chaulk and A. M. MacMillan, *Nat. Protoc.*, 2007, **2**, 1052–1058.

19 I. A. Shestopalov, S. Sinha and J. K. Chen, *Nat. Chem. Biol.*, 2007, **3**, 650–651.

20 P. K. Jain, S. Shah and S. H. Friedman, *J. Am. Chem. Soc.*, 2011, **133**, 440–446.
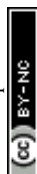
21 J. Hemphill, Q. Y. Liu, R. Uprety, S. Samanta, M. Tsang, R. L. Juliano and A. Deiters, *J. Am. Chem. Soc.*, 2015, **137**, 3656–3662.

22 Y. Z. Ji, J. L. Yang, L. Wu, L. J. Yu and X. J. Tang, *Angew. Chem., Int. Ed.*, 2016, **55**, 2152–2156.

23 P. K. Jain, V. Ramanan, A. G. Schepers, N. S. Dalvie, A. Panda, H. E. Fleming and S. N. Bhatia, *Angew. Chem., Int. Ed.*, 2016, **55**, 12440–12444.

24 W. A. Velema, A. M. Kietrys and E. T. Kool, *J. Am. Chem. Soc.*, 2018, **140**, 3491–3495.

25 S. Wang, L. Wei, J.-Q. Wang, H. Ji, W. Xiong, J. Liu, P. Yin, T. Tian and X. Zhou, *ACS Chem. Biol.*, 2020, **15**, 1455–1463.

26 S. R. Wang, L. Y. Wu, H. Y. Huang, W. Xiong, J. Liu, L. Wei, P. Yin, T. Tian and X. Zhou, *Nat. Commun.*, 2020, **11**, 91.

27 Y. Liu, R. S. Zou, S. X. He, Y. Nihongaki, X. G. Li, S. Razavi, B. Wu and T. Ha, *Science*, 2020, **368**, 1265–1269.

28 E. V. Moroz-Omori, D. Satyapertiwi, M. C. Ramel, H. Hogset, I. K. Sunyovszki, Z. Q. Liu, J. P. Wojciechowski, Y. Y. Zhang, C. L. Grigsby, L. Brito, L. Bugeon, M. J. Dallman and M. M. Stevens, *ACS Cent. Sci.*, 2020, **6**, 695–703.

29 W. Y. Zhou, W. Brown, A. Bardhan, M. Delaney, A. S. Ilk, R. R. Rauen, S. I. Kahn, M. Tsang and A. Deiters, *Angew. Chem., Int. Ed.*, 2020, **59**, 8998–9003.

30 Y. Zhang, X. Y. Ling, X. X. Su, S. L. Zhang, J. Wang, P. J. Zhang, W. J. Feng, Y. Y. Zhu, T. Liu and X. J. Tang, *Angew. Chem., Int. Ed.*, 2020, **132**, 21081–21085.

31 Y. Ochi, O. Nakagawa, K. Sakaguchi, S. Wada and H. Urata, *Chem. Commun.*, 2013, **49**, 7620–7622.

32 Y. Ochi, M. Imai, O. Nakagawa, J. Hayashi, S. Wada and H. Urata, *Bioorg. Med. Chem. Lett.*, 2016, **26**, 845–848.

33 I. Khan, L. M. Seebald, N. M. Robertson, M. V. Yigit and M. Royzen, *Chem. Sci.*, 2017, **8**, 5705–5712.

34 A. Kadina, A. M. Kietrys and E. T. Kool, *Angew. Chem., Int. Ed.*, 2018, **57**, 3059–3063.

35 M. Habibian, C. McKinlay, T. R. Blake, A. M. Kietrys, R. M. Waymouth, P. A. Wender and E. T. Kool, *Chem. Sci.*, 2020, **11**, 1011–1016.

36 R. C. Spitale, P. Crisalli, R. A. Flynn, E. A. Torre, E. T. Kool and H. Y. Chang, *Nat. Chem. Biol.*, 2013, **9**, 18–20.

37 W. A. Velema and E. T. Kool, *Nat. Rev. Chem.*, 2020, **4**, 22–37.

38 P. K. Jain, V. Ramanan, A. G. Schepers, N. S. Dalvie, A. Panda, H. E. Fleming and S. N. Bhatia, *Angew. Chem., Int. Ed.*, 2016, **55**, 12440–12444.

39 W. Zhou and A. Deiters, *Angew. Chem., Int. Ed.*, 2016, **55**, 5394–5399.

40 F. Richter, I. Fonfara, R. Gelfert, J. Nack, E. Charpentier and A. Moglich, *Curr. Opin. Biotechnol.*, 2017, **48**, 119–126.

41 R. Galizi and A. Jaramillo, *Curr. Opin. Biotechnol.*, 2019, **55**, 103–113.

42 W. Tang, J. H. Hu and D. R. Liu, *Nat. Commun.*, 2017, **8**, 15939.

43 K. Kundert, J. E. Lucas, K. E. Watters, C. Fellmann, A. H. Ng, B. M. Heineike, C. M. Fitzsimmons, B. L. Oakes, J. Qu, N. Prasad, O. S. Rosenberg, D. F. Savage, H. El-Samad, J. A. Doudna and T. Kortemme, *Nat. Commun.*, 2019, **10**, 2127.

44 X. W. Wang, L. F. Hu, J. Hao, L. Q. Liao, Y. T. Chiu, M. Shi and Y. Wang, *Nat. Cell Biol.*, 2019, **21**, 522–530.

45 S. L. Beaucage, *Curr. Opin. Drug Discovery Dev.*, 2008, **11**, 203–216.

46 M. Flamme, L. K. McKenzie, I. Sarac and M. Hollenstein, *Methods*, 2019, **161**, 64–82.

47 D. Trachootham, J. Alexandre and P. Huang, *Nat. Rev. Drug Discovery*, 2009, **8**, 579–591.

48 S. J. Dixon and B. R. Stockwell, *Nat. Chem. Biol.*, 2014, **10**, 9–17.

49 C. Nathan and A. Cunningham-Bussel, *Nat. Rev. Immunol.*, 2013, **13**, 349–361.

50 S. Mori, K. Morihiro, T. Okuda, Y. Kasaharaa and S. Obika, *Chem. Sci.*, 2018, **9**, 1112–1118.

51 L. Xiao, C. Gu and Y. Xiang, *Angew. Chem., Int. Ed.*, 2019, **58**, 14167–14172.

52 C. Menge and A. Heckel, *Org. Lett.*, 2011, **13**, 4620–4623.

53 S. W. Wright, D. L. Hageman and L. D. McClure, *J. Org. Chem.*, 1994, **59**, 6095–6097.

54 S. Yamaguchi, S. Akiyama and K. Tamao, *J. Am. Chem. Soc.*, 2001, **123**, 11372–11375.

55 D. Zhang, C. Y. Zhou, K. N. Busby, S. C. Alexander and N. K. Devaraj, *Angew. Chem., Int. Ed.*, 2018, **57**, 2822–2826.

56 D. Zhang, S. Jin, X. Piao and N. K. Devaraj, *ACS Chem. Biol.*, 2020, **15**, 1773–1779.

57 S. Shah, S. Rangarajan and S. H. Friedman, *Angew. Chem., Int. Ed.*, 2005, **44**, 1328–1332.

58 S. Shah, P. K. Jain, A. Kala, D. Karunakaran and S. H. Friedman, *Nucleic Acids Res.*, 2009, **37**, 4508–4517.

59 F. Eckstein, *Nucleic Acid Ther.*, 2014, **24**, 374–387.

60 J. A. Fidanza, H. Ozaki and L. W. Mclaughlin, *J. Am. Chem. Soc.*, 1992, **114**, 5509–5517.

61 M. N. Stojanovic, E. G. Green, S. Semova, D. B. Nikic and D. W. Landry, *J. Am. Chem. Soc.*, 2003, **125**, 6085–6089.

62 J. H. Lee, D. P. Wernette, M. V. Yigit, J. Liu, Z. Wang and Y. Lu, *Angew. Chem., Int. Ed.*, 2007, **46**, 9006–9010.

63 L. H. Tan, H. Xing and Y. Lu, *Acc. Chem. Res.*, 2014, **47**, 1881–1890.

64 W. Zhou, F. Wang, J. Ding and J. Liu, *ACS Appl. Mater. Interfaces*, 2014, **6**, 14795–14800.

65 Y. Guo, J. Zhang, F. Ding, G. Pan, J. Li, J. Feng, X. Zhu and C. Zhang, *Adv. Mater.*, 2019, **31**, 1807533.

66 J. Zhang, Y. Guo, F. Ding, G. Pan, X. Zhu and C. Zhang, *Angew. Chem., Int. Ed.*, 2019, **58**, 13794–13798.

67 Y. Guo, J. Zhang, G. Pan, C. H. J. Choi, P. Wang, Y. Li, X. Zhu and C. Zhang, *Chem. Commun.*, 2020, **56**, 7439–7442.

68 X. Y. Wang, M. L. Feng, L. Xiao, A. J. Tong and Y. Xiang, *ACS Chem. Biol.*, 2016, **11**, 444–451.

69 M. L. Feng, Z. Y. Ruan, J. C. Shang, L. Xiao, A. J. Tong and Y. Xiang, *Bioconjugate Chem.*, 2017, **28**, 549–555.

70 D. Kawaguchi, A. Kodama, N. Abe, K. Takebuchi, F. Hashiya, F. Tomoike, K. Nakamoto, Y. Kimura, Y. Shimizu and H. Abe, *Angew. Chem., Int. Ed.*, 2020, **59**, 17403–17407.

71 Y. Wu, Y. Tang, X. Dong, Y. Y. Zheng, P. Haruehanroengra, S. Mao, Q. Lin and J. Sheng, *ACS Chem. Biol.*, 2020, **15**, 1301–1305.

72 Y. L. Chiu and T. M. Rana, *RNA*, 2003, **9**, 1034–1048.

73 C. Behl, J. B. Davis, R. Lesley and D. Schubert, *Cell*, 1994, **77**, 817–827.

74 M. Horoz, C. Bolukbas, F. F. Bolukbas, M. Aslan, A. O. Koylu, S. Selek and O. Erel, *BMC Infect. Dis.*, 2006, **6**, 114.

75 R. Weinstain, E. N. Savariar, C. N. Felsen and R. Y. Tsien, *J. Am. Chem. Soc.*, 2014, **136**, 874–877.

76 S. H. Sternberg, S. Redding, M. Jinek, E. C. Greene and J. A. Doudna, *Nature*, 2014, **507**, 62–67.

77 R. D. Mashal, J. Koontz and J. Sklar, *Nat. Genet.*, 1995, **9**, 177–183.

78 E. K. Brinkman, T. Chen, M. Amendola and B. van Steensel, *Nucleic Acids Res.*, 2014, **42**, e168.

79 C. T. Dooley, T. M. Dore, G. T. Hanson, W. C. Jackson, S. J. Remington and R. Y. Tsien, *J. Biol. Chem.*, 2004, **279**, 22284–22293.

80 M. Malinouski, Y. Zhou, V. V. Belousov, D. L. Hatfield and V. N. Gladyshev, *PLoS ONE*, 2011, **6**, e14564.

81 M. F. Sentmanat, S. T. Peters, C. P. Florian, J. P. Connelly and S. M. Pruett-Miller, *Sci. Rep.*, 2018, **8**, 888.

82 A. J. Mahiny, A. Dewerth, L. E. Mays, M. Alkhaled, B. Mothes, E. Malaeksefat, B. Loretz, J. Rottenberger, D. M. Brosch, P. Reautschnig, P. Surapolchai, F. Zeyer, A. Schams, M. Carevic, M. Bakele, M. Griese, M. Schwab, B. Nurnberg, S. Beer-Hammer, R. Handgretinger, D. Hartl, C. M. Lehr and M. S. Kormann, *Nat. Biotechnol.*, 2015, **33**, 584–586.

83 H. Yin, C. Q. Song, J. R. Dorkin, L. J. Zhu, Y. Li, Q. Wu, A. Park, J. Yang, S. Suresh, A. Bizhanova, A. Gupta, M. F. Bolukbasi, S. Walsh, R. L. Bogorad, G. Gao, Z. Weng, Y. Dong, V. Koteliansky, S. A. Wolfe, R. Langer, W. Xue and D. G. Anderson, *Nat. Biotechnol.*, 2016, **34**, 328–333.

84 P. Perez-Pinera, D. D. Kocak, C. M. Vockley, A. F. Adler, A. M. Kabadi, L. R. Polstein, P. I. Thakore, K. A. Glass, D. G. Ousterout, K. W. Leong, F. Guilak, G. E. Crawford, T. E. Reddy and C. A. Gersbach, *Nat. Methods*, 2013, **10**, 973–976.

85 L. S. Qi, M. H. Larson, L. A. Gilbert, J. A. Doudna, J. S. Weissman, A. P. Arkin and W. A. Lim, *Cell*, 2013, **152**, 1173–1183.

86 N. M. Gaudelli, A. C. Komor, H. A. Rees, M. S. Packer, A. H. Badran, D. I. Bryson and D. R. Liu, *Nature*, 2017, **551**, 464–471.

87 D. B. T. Cox, J. S. Gootenberg, O. O. Abudayyeh, B. Franklin, M. J. Kellner, J. Joung and F. Zhang, *Science*, 2017, **358**, 1019–1027.

88 N. Iwamoto, D. C. D. Butler, N. Svrzikapa, S. Mohapatra, I. Zlatev, D. W. Y. Sah, Meena, S. M. Standley, G. Lu, L. H. Apponi, M. Frank-Kamenetsky, J. J. Zhang, C. Vargeese and G. L. Verdine, *Nat. Biotechnol.*, 2017, **35**, 845–851.

89 K. W. Knouse, J. N. deGruyter, M. A. Schmidt, B. Zheng, J. C. Vantourout, C. Kingston, S. E. Mercer, I. M. McDonald, R. E. Olson, Y. Zhu, C. Hang, J. Zhu, C. Yuan, Q. Wang, P. Park, M. D. Eastgate and P. S. Baran, *Science*, 2018, **361**, 1234–1238.

90 T. C. Roberts, R. Langer and M. J. A. Wood, *Nat. Rev. Drug Discovery*, 2020, **19**, 673–694.